

Differentiation of Monkeypox from Other Poxes Using Local Interpretable Model-Agnostic Explanation and Deep Learning Algorithm

Anietie Ekong¹, Unyime Edet², Gabriel James³, David Igweze⁴

^{1&2}Department of Computer Science, Akwa Ibom State University, Nigeria

³Department of Computing, Topfaith University, Mkpatak, Nigeria

⁴Department of Instrumentation and Control Systems, Dangote Petroleum Refinery and Petrochemicals FZE, Lagos, Nigeria

ABSTRACT

While still trying to recover from the harm brought by COVID-19, the pox virus, particularly MPox (Monkeypox), now poses a fresh threat of spreading to the entire world. Skin lesions and rashes caused by Mpox are similar to such caused by other pox diseases such as chickenpox and cowpox and these medical and visual resemblances of several pox diseases make it difficult for healthcare providers to establish an early diagnosis leading to inefficient control of the disease's transmission within a community. In image-based diagnostics, deep learning has shown enormous potential. However, there exist the challenges of complexity of the model and lack of understanding of the prediction parameters for making classification and inference. In this research, a machine learning approach for the classification of Mpox from other pox diseases is proposed. The dataset was created by compiling images from open-source and internet resources that place no limitations on usage. Three models were proposed and evaluated: the CNN model, ResNet50, and EfficientNetNB. Two of the models were pre-trained models while the CNN model was developed completely new. During testing, the CNN model was the best-performing model outperforming state-of-the-art pre-trained models. Our experimentation using the test dataset indicated that our Convolutional Neural Network (CNN) model can identify six classes of skin images with 99% accuracy, 98% precision score, 99% recall, and 98% F1 score. The AUC score of our CNN model was obtained as 99%. Finally, the use of Local Interpretable Model-Agnostic Explanations (LIME) was used to provide meaningful insight into how the CNN the best-performing model among the three arrived at a particular decision based on the extracted feature from the input data.

Keywords: Diseases diagnosis, Bio-inspired computing, Computer vision, Machine learning, Agnostic explanations, Convolutional neural network, Medical image diagnostics, Monkeypox, Pox

INTRODUCTION

Pox viruses are the cause of a wide range of pox diseases in animals and humans. While clinically less severe than smallpox, Mpox also known as monkeypox is a viral zoonosis with symptoms comparable to those of smallpox, WHO (2022). The possibility of a worldwide pandemic from the Mpox virus has emerged as the world struggles to recover from the harm caused by COVID-19. According to Shchelkunov et al. (2002), the Mpox virus belongs to the Orthopoxvirus of the Poxviridae family and was initially transmitted from animals to humans. In Nigeria, for example, according to CDC (2022), 704 cases have been detected from 1st January to 28th August 2022.

Initial observations of the distinct characteristics of the skin lesions and rashes present, as well as the history of exposure, are part of the Mpox diagnostic procedures. However, employing electron microscopy to examine skin lesions remains one of the best techniques to

identify the virus. Deep learning techniques have in recent times proven to be very effective in medical diagnosis and have wide-reaching solutions including the classification of pox diseases. With an established ability to handle decision-making, industrial processes, diagnostic systems, etc, machine learning (ML) is an emerging field of artificial intelligence (AI). Clinicians achieve safe, reliable, and universally recognized imaging solutions using the abilities of ML. While the effectiveness of these solutions cannot be underestimated, there is increasing demand for some explainability and interpretability of machine learning models. LIME focuses on developing neighborhood surrogate models to justify specific predictions and on training local surrogate models rather than creating a global surrogate model, Ribeiro et al (2016). LIME can be applied to any ML model. By changing the data samples fed into the system and keenly observing the predictive variations, it objectively attempts to explain the model. Although using deep learning models has proven to be effective and efficient in accurately classifying images into different classes, they, however, pose the challenges of the complexity of the model and lack of understanding of the prediction parameters used by the model for making classification and inference. The medical and visual resemblance of several pox diseases makes it difficult for healthcare providers to establish an early diagnosis of Mpox. Mpox infection has a low death rate (1%–10%) WHO (2022), but lack of early diagnosis of the disease will hamper patient isolation and contact tracing leading to inefficient control of the disease's transmission within a community.

Four processes make up the usual Computer Aided Diagnostic (CAD) system's workflow for medical image analysis: image pre-processing, segmentation, feature extraction and selection, and lesion classification and the use of CAD technologies can ensure timeous and accurate diagnoses. This study therefore seeks to provide a solution for differentiating Mpox from other pox diseases by skin images presented using CNN, a deep learning algorithm, and LIME.

LITERATURE REVIEW

Various new and re-emerging infections as well as a wide variety of dreaded and deadly infectious diseases in humans and animals continue to be caused by viruses. Comparatively speaking, they provide a significantly bigger threat to global public health now than they did a century ago. As the world was gearing up to commemorate decades of smallpox eradication, some countries like Nigeria recently saw an epidemic of a severe skin rash condition that resembles both varicella zoster and smallpox. The etiologic agent for this outbreak is the Mpox virus (MPXV). According to WHO (2022), Mpox poses moderate health concern and its fast spread to nations with negligible epidemiological ties to endemic regions demands attention.

Several factors contribute to the re-emergence of this dreaded disease and the factors include urbanization and poaching, increasing demand for and consumption of wildlife animals, young population, floods and torrential rainfall place MPXV-infected animal hosts and people close together, and HIV co-infection-related immune suppression

Clinical Characteristics and Diagnosis of Mpox Virus

According to Lundervold and Lundervold (2019), deep neural networks are widely deployed in learning models from image analysis to natural language processing (NLP). These have a huge positive impact on medical imaging technology and healthcare in general. By identifying patterns in the digital images, mostly on the skin, this study will allow for the categorization of skin lesions and rashes quickly and effectively as being Mpox or not.

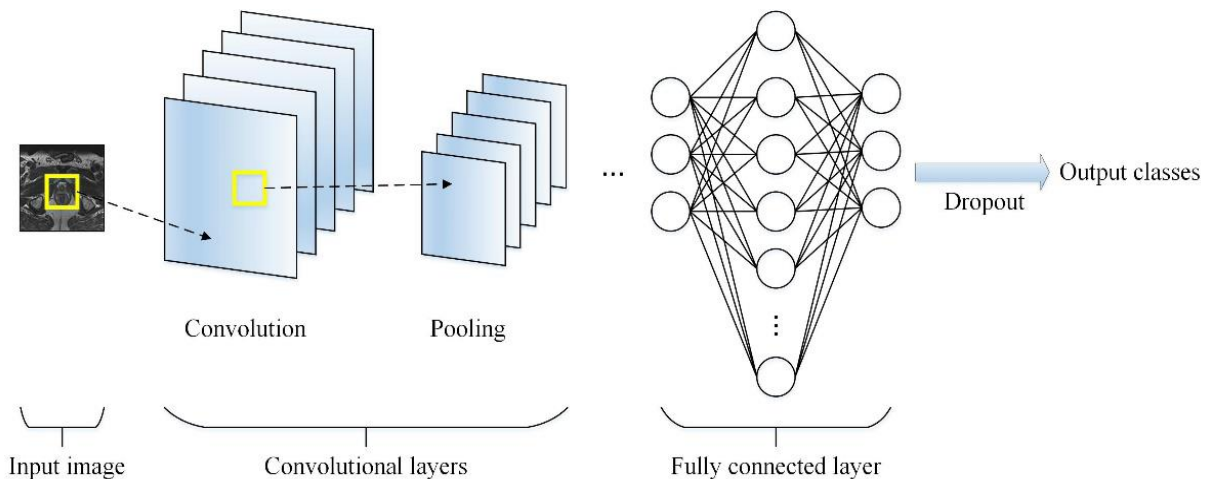


Figure 1: An Example of CNN Framework for Image Classification (Gao et al., 2019)

Convolutional Neural Network and Its Application on Medical Diagnosis

According to Gao et al. (2019), Medical imaging has steadily developed into a critical component of precision medicine and has become essential for the identification or diagnosis of illnesses, particularly for the diagnosis of malignancies. Manual data interpretation and analysis have steadily grown difficult due to the advancement of science and technology applications in medical imaging leading to radiologists who may misunderstand symptoms, resulting in missed diagnoses (false negative findings), the interpretation of non-lesions as lesions, or the interpretation of benign lesions as malignant (false positive results).

The CNN-based approach is one of the approaches used for deep learning. A typical CNN architecture (shown in Figure 1) is made up of one or more fully linked layers, one or more pooling layers, and one or more convolution layers Gao et al. (2019).

To identify fibrillations and flutters, the most prevalent kind of clinically diagnosed arrhythmia, Fujita et al. (2019) created a revolutionary deep neural network-based architecture. According to their research, the suggested CNN could identify arrhythmias well. Afonso et al. (2019) employed recurrence plots to map the motor signals onto the picture domain to automatically diagnose Parkinson's disease, which was then used to feed a CNN. Compared to their prior research, experimental findings significantly improved, with an average accuracy of nearly 87%.

CADx which is used to refer to medical image analysis activities including classification, characterization, identification, and diagnosis requires not only the identification of worrisome lesions but also their characterization and categorization. In their work, Ahmad et al. (2019) compiled data supporting the clinical uses of CADx and AI in colonoscopy. A CAD system named DermaKNet was introduced by Gonzalez-Diaz et al. (2019) for the diagnosis of skin lesions. The authors sought to get beyond the typical deep learning constraint regarding the interpretability of the findings by adding the specialist information offered by dermatologists into the decision-making process. According to the research, segmentation and diagnostic networks may be combined into end-to-end trainable architectures thanks to multi-task losses.

To accurately diagnose glaucoma in 2018, Raghavendra et al. (2018) trained an 18-layer CNN to extract strong characteristics from the digital fundus pictures. They achieved an accuracy of 98.13% with a very modest data set, demonstrating the capabilities of CAD systems.

Ekong (2023) evaluated the effectiveness of ML algorithms: K-Nearest Neighbour(KNN), Support Vector Machine (SVM), and Random Forest (RF) for the diagnosis of heart diseases. The results showed accuracies of KNN, SVM, and RF as 0.8, 0.7889, and

0.76670 respectively. This further stressed the importance of machine learning in disease diagnoses

To enhance the prediction of Alzheimer's disease, Hosseini-Asl et al. (2018) suggested a three-dimensional CNN (3D-CNN), which could display general characteristics retrieved from brain pictures, adapted to varied domain datasets and effectively classify the pictures into different datasets. The results from their experiments showed that this method performed better than previous CNN-based techniques and traditional classifiers. Deep learning algorithms were able to do this task since diagnosing Alzheimer's disease in older patients was challenging and required a highly discriminative feature representation for classification. A 98.8% accuracy was achieved while performing the experimental findings on the dataset.

Zhao et al. (2018) developed an agile CNN framework to handle the issues of small-scale medical image databases and pulmonary nodule classification showed a remarkable improvement using CT images.

Allugunti (2022) proposed a technique for segmenting thermal imaging breast pictures and detecting breast cancer, which was accurate and effective. This technique allows the images to be classified as normal or pathological. CNN was used to perform analysis and classification of the segmented thermographic pictures. Infrared images of healthy persons and those with cancer were evaluated. A total of 1000 images of patients with and without breast cancer, 99.65% overall accuracy was obtained with a training loss of 0.0067. When compared with the traditional ML algorithm such as the SVM, an overall accuracy of 89.84% was obtained, showing that the deep learning model certainly performed better.

Naseen et al. (2022) proposed an ensemble method which consisted of four ML algorithms. All four models were stacked or ensemble and fed to Artificial Neural Network for final classification. The support vector machine model had an average accuracy score of 98.10% closely followed by the logistic regression for the diagnosis. On the side of detection or prognosis, the same support vector machine had an average score of 78.35% followed by random forest.

A segmentation-free strategy to identify benign and malignant breast cancers using CNN was described by Zhou et al. (2018). 95.7% was obtained as the accuracy 96.2% as the sensitivity, and 95.7% as specificity, and the model was trained on 540 photos, which was a good result. Additionally, it was the first attempt to automatically extract high-throughput characteristics from shear wave elastography data to categorize breast cancers using radionics based on CNN.

In a bit to discriminate multiclass concerning types of tissue, a bilinear CNN deep learning model for classification and generation of prediction map for automatic tissue segmentation was proposed by Xu et al. (2022). They suggested an easy-to-use but efficient technique that integrated Bilinear-CNN to make output fluctuations relatively significant across classes. Due to its remarkable performance in computer vision tests, ResNet50 was the component of the network from which the features were extracted. Compared to pre-trained ResNet50, they eliminated the global average pooling layer. Instead, a bilinear pooling module received the characteristics the convolution layer had extracted. The characteristics that reflected the importance of the components of the tissue, the output of the bilinear pooling module, were then included as a soft attention module and utilized to receive the bilinear pooling module's output. They used Grad-CAM to produce the interpretability of the classification to show that the CNN-based model can differentiate the tissue types.

Using user-taken skin photos, Ali et al. (2022) established a binary categorization of Mpox and other skin illnesses. Several convolutional neural network models, including VGG-16, ResNet50, and Inception-V3 were put to the test by the authors. The dataset excludes photographs of healthy skin tissue and utilizes 102 images of Mpox and 126 images of other skin illnesses. The classifier accuracy was evaluated to be 82%.

Ahsan et al. (2022) made use of a bespoke dataset made up of the four classes healthy, measles, chickenpox, and Mpox, each of which has 54, 17, 47, and 43 photos. The collection is highly imbalanced and contains relatively few photos for several classes in addition to the author's use of a data augmentation procedure. However, just two classes, Mpox versus others and Mpox versus chickenpox were used in training the created classifiers. The authors achieve an accuracy of 83% for the Mpox versus others for the training subset and an accuracy of 78% for the second experiment utilizing the training subset while employing a VGG-16 CNN for each implemented system.

To get automated classification results between healthy, mpox, and other skin damages, given a close-up photograph of the skin tissue, Munoz-Saavedra et al. (2022) created and assessed classifiers based on Convolutional Neural Network models and various ensembles comprising of combination of such models. They gathered Mpox images from public datasets, pictures of healthy people, and people with other skin diseases. They created, implemented, and evaluated several Mpox disease diagnostic and detection algorithms using these photos. Given a close-up photograph of the skin tissue, the classifiers were constructed and assessed based on Convolutional Neural Network models and some ensembles made up of a mixture of those models, yielding automated classification results between healthy, Mpox, and other skin damages. When utilizing a specific CNN model (VGG-19 and ResNet50), the findings revealed a system accuracy of more than 93%, and when using a CNN ensemble made up of ResNet50, EfficientNet-B0, and MobileNet-V2, the results revealed a system accuracy of more than 98%. Figure 2 shows their system implementation framework.

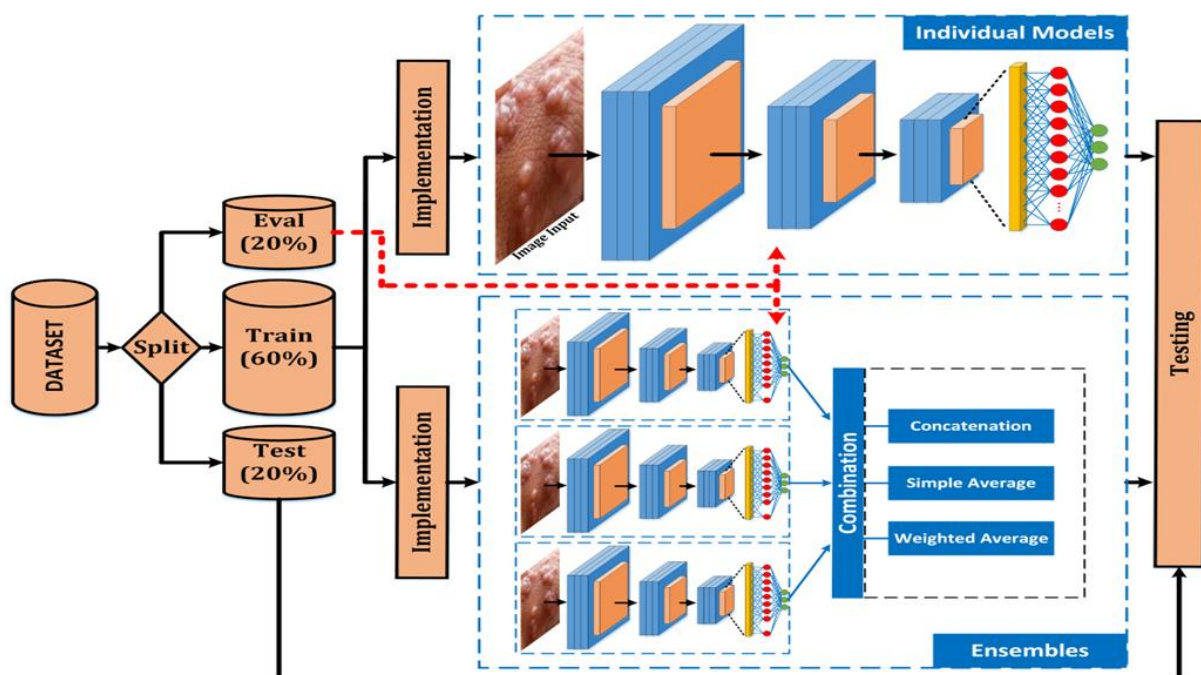


Figure 1 (Muñoz-Saavedra et al., 2022)

The issue with the problem of employing AI for Mpox detection has been the scarcity of Mpox skin imaging data. The Mpox Skin Image Dataset 2022, published by Hussain et al. in 2022 using 804 unique pox images investigated the viability of detecting Mpox on skin photos using cutting-edge AI deep models. After getting a precision score of 85%, they concluded that AI models had significant promise in identifying Mpox from pictures of the skin but that larger training data were needed to get better detection accuracy.

To circumvent the issue of limited access or lack of publicly available datasets, especially in the area of health and medical science which can impact negatively the development of deep

learning models, Ekong et al. (2022) adopted a traditional machine learning approach based on Bayesian Belief Network for the classification of symptoms of Covid-19 patients. In their work, an accuracy of 98% was achieved during the classification of patients' symptoms on the test data as CoV+ or CoV-.

By analyzing patients' hyperspectral photos, Jeyaraj et al. (2019) created an automated and computer-aided oral cancer diagnostic method. An accuracy, sensitivity, and specificity of 94.5%, 94.0%, and 98.0% respectively were achieved in their study using the regression-based partitioned approach. Since no specialized expertise was required, the suggested system could be quickly created on a basic workbench in practice.

A Deep Convolutional Neural Network (DCNN) based on transfer learning to reduce the decrease of false positives in the detection of lung nodules was proposed by Shi et al. (2019). Lung nodules were categorized using SVM, while discriminative features were extracted with VGG-16. The sensitivity was high enough for applications, reaching 87.2% with 0.39 false positives for every run.

Muñoz-Saavedra et al. (2022) used a very small data sample comprising 100 images of healthy skin, 100 images of pox-infected skin, and 100 images of other related skin diseases. Such a low sample of data points can impact the results of the model negatively which also affects the validity and reliability of the results due to the limited spread of the dataset. Their framework is shown in Figure 2.

Using a large dataset of dermatoscopic image data from different sources to train the model will surely increase the accuracy of the system and providing some interpretability of the classifier provides some insights into the model decision-making skill is necessary and is part of what we intend to achieve.

Model and Interpretability

Since most studies only aim for the greatest accuracy metrics in their tasks, the subject of explainability in healthcare has gone unaddressed for a long time. Several frameworks for interpreting image classification have been put out by Petsiuk et al. (2018) and Lundberg et al. (2017) and they can be used for medical images too. There are comprehensible models for Alzheimer's and Parkinson's disease categorization, created by Das et al. (2019), Magesh et al. (2020), and many others but few for Monkeypox (Mpox) illness. This research seeks to develop a comprehensible model for the same to bridge that gap.

RESEARCH METHODOLOGY

Artificial neural networks (ANN) with several layers are referred to as deep learning or deep neural networks. CNN is one of the most popular deep neural networks. Convolutional, non-linear, pooling and fully connected layers are among the many layers that make up CNN (James, et al., 2024a; Ekong, et al., 2024b; James, et al., 2024c). Pooling and non-linearity layers lack parameters, but convolutional and fully connected layers do. In machine learning problems, the CNN performs quite well. Particularly the image-related applications, computer vision, and NLP, the performance attained by CNN is truly astounding. Reducing the number of ANN parameters is the main advantage of employing CNNs. In the fully connected layer, neurons are grouped similarly to how they are in an artificial neural network. As a result, any node in a layer that is completely linked is directly connected to every node in the layer above it as well as the layer below it. Using the dropout approach, an effort is made to reduce the quantity of nodes and connections. The proposed model framework is shown in Figure 3.

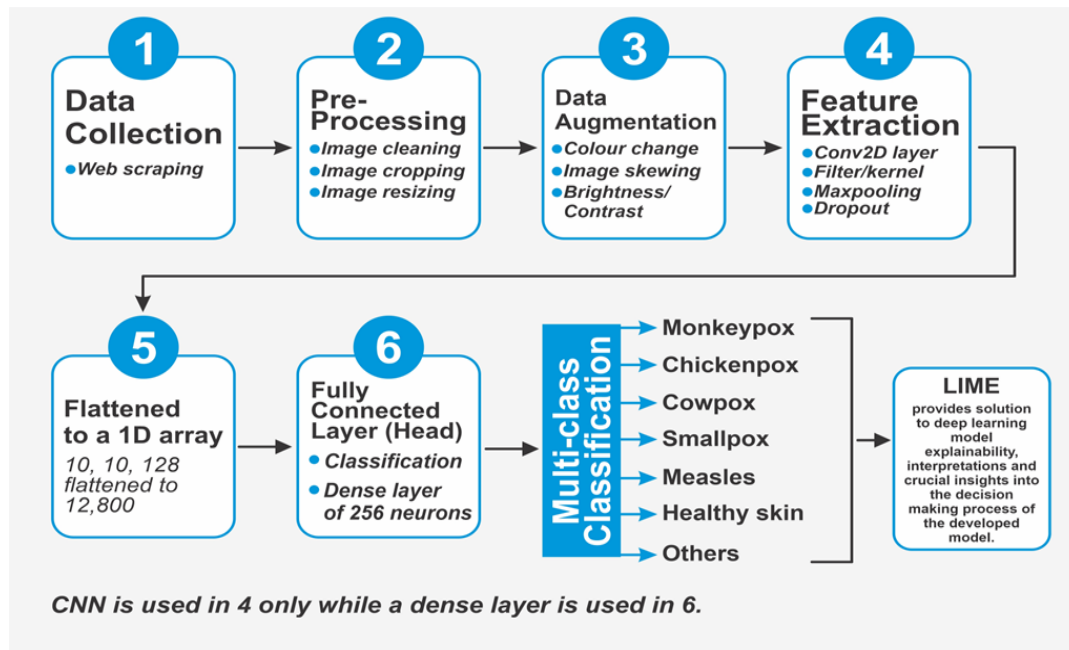


Figure 3: Proposed Model Framework

Analysis of Key Phases/Components of the Proposed Framework

1. Data Collection

Artificial Intelligence (AI) systems need large data to function effectively. Digital picture dataset of rashes or skin lesions caused by Mpox, measles, chickenpox, smallpox, cowpox, and Mpox.

2. Data Augmentation

To prevent overfitting, CNN significantly relies on massive data with the necessary spread. Sadly, many application fields lack access to big data, including the interpretation of medical images. The term data augmentation refers to a technique used to increase the training datasets by the development of modified datasets from existing datasets to make the models more robust. Using the freshly augmented images, the model was trained and fine-tuned to increase its effectiveness. Using the Keras image data generator technique, we added 14 augmentation processes to the images to boost their quantity and provide variety to the data.

The augmentation processes include the following:

- I. Modification of the brightness with a randomly generated factor of 0.5 to 2
- II. Modification of the color of the images randomly using a factor of 0.5 to 1.5
- III. The sharpness of the images was modified randomly in the range of 0.5 to 2.
- IV. Image translation along the width and height by randomly transforming it between -20 and 20 pixels in both directions.
- V. Image shearing of the original data collected using random parameters
- VI. Addition of variance in the range of 0.005 to 0.02 and Gaussian noise and zero mean to the image dataset.
- VII. Zero mean speckle noise and 0.005 to 0.02 range of randomly generated variance was added to the image dataset.
- VIII. Modifying image pixel values using local variance.
- IX. Randomly generated salt noise in the range of 2 and 8 percent was added to the images
- X. Blurring of images by applying Gaussian kernel blur with randomly generated values ranging from 1 to 3 pixels.
- XI. Image rotation was done on the dataset by randomly rotating all images by 90°.

XII. More rotation was applied to the images by rotating them in the range of -45 to 45 degrees.

XIII. Zooming in an image was applied to the dataset.

XIV. Flipping of images along the width and height was applied to the dataset.

The CNN pipeline is shown in Figure 4. Sample images grouped according to their classes are shown in Figure 5.

Cleaning, filtering, and manipulating raw data as well as locating and classifying missing values are all parts of the process known as data preprocessing. Raw data must be processed to be transformed into a machine learning-friendly format. To extract information and infer meanings from raw data and to better comprehend the events that produced the data, preprocessing requires transforming the raw data into a format and structure that may be utilized for these purposes. The following data preparation methods were used: data cleaning, image cropping, and image color transformation. For privacy's sake, undesirable background areas and intimate areas were cropped while the eyes were masked. Extra blank pixels in the perimeter of many photographs were added to prevent or reduce the stretching effect. Finally, we used bilinear interpolation to crop and resize each image to 128 x 128 x 3 pixels.

Model's Algorithm

1. Collect images of mpox and other pox diseases such as chickenpox, smallpox, cowpox, and measles
2. Collect image data into different folders grouped according to the type of poxvirus. Distance images or whole-body images are excluded from the dataset.
3. Subject image dataset to screening to validate the dataset.
4. Apply data preprocessing techniques such as cropping of images to the standard size of 224x224x3 pixel values required by pre-trained CNN models. The cropped images remove unwanted regions and block out black boxes.
5. Apply data augmentation of the dataset to increase the number of training samples which also introduces variability into the dataset.

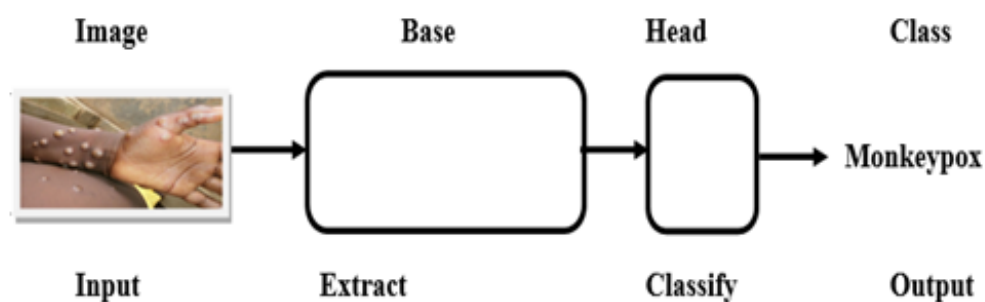


Figure 4: Variability in the dataset

6. Implement ResNet50, VGG16, and MobileNet-v2 Deep Models framework.
7. Use cross-validation for fine-tuning deep models as well as adjusting the learning rate and introducing early stoppage criteria.
8. Schedule fine-tuning each deep model for specific epochs/folds.



Figure 5: Sample Images of dataset

9. Select the best validation score for each fold
10. Use Adam optimizer, batch size of 16 in addition to 0.0001 as the learning rate.

Model Training and Testing

The model is built in Python using Keras. Fine-tuning of model parameters is done after each image has been resized. The following parameters are used for data augmentation: rotation range=50, rescale=1/255, width shift range=0.2, height shift range=0.2, shear range=0.25, zoom range=0.1, and channel shift range=20. Adam optimizer is used while the batch size is set to 16, plus the learning rate is set at 0.0001. To solve the problem of overfitting, we use the learning rate decay on every epoch in conjunction with early-stopping criteria, and a random five-fold (5-cross validation) is used. The images in the dataset are used to train the classifiers, with 80% of the images utilized for training and the remaining 20% for testing. Sample images of the dataset. The class distribution of the dataset is presented in Table 1.

Table 1: Class distribution of the dataset

Class of Disease	Original Images	Augmented Images
Chickenpox	234	9500
Cowpox	60	3426
Measles	50	2207
Mpox	217	6058
Healthy	60	3502
Smallpox	300	16520
Total	921	41213

- i. The Convolutional Classifier
- ii. Model Training Evaluation

RESULTS AND DISCUSSION

Figure 6 to Figure 11 shows the graph of loss/accuracy during training of the three deep learning models.

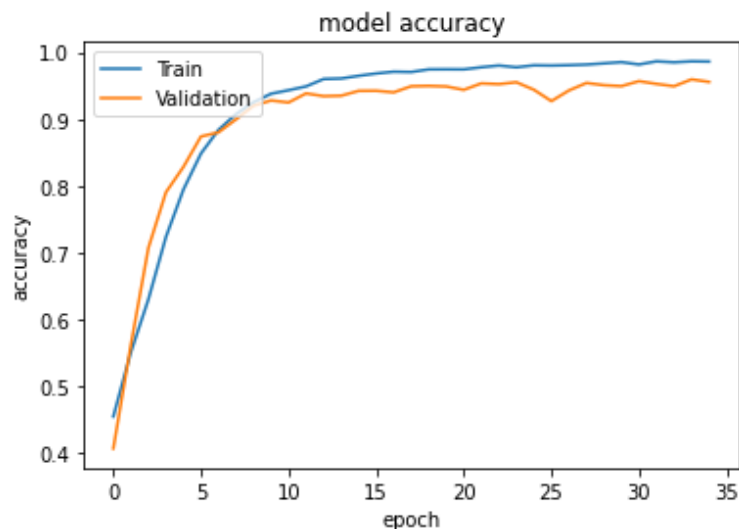


Figure 6: CNN Model accuracy for training and validation sets

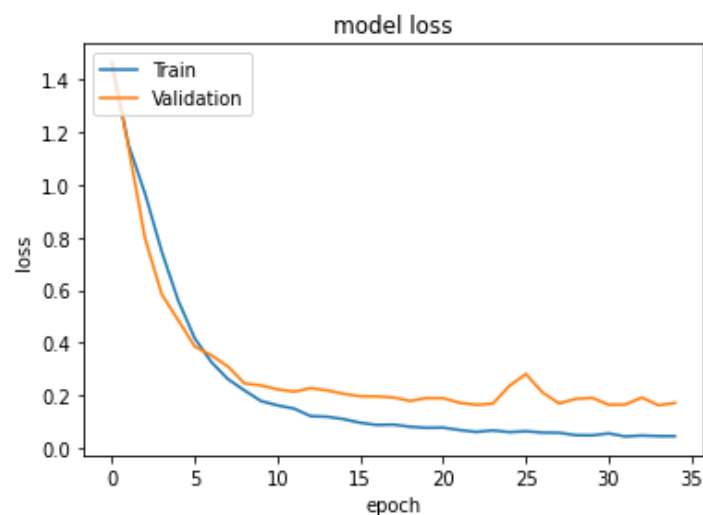


Figure 7: CNN model loss for training and validation loss

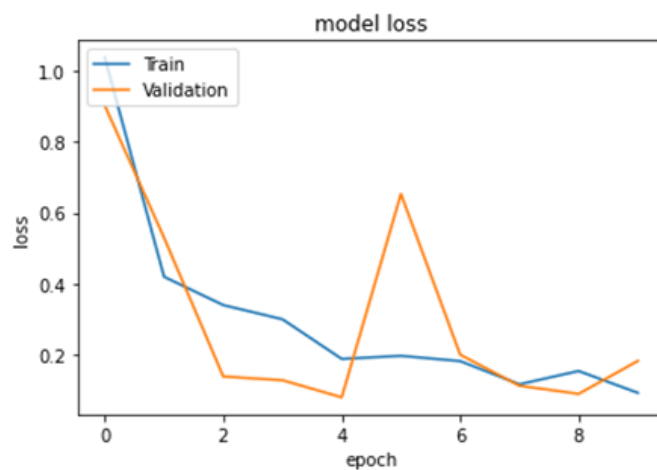


Figure 8: EfficientNetNB model loss for training and validation loss

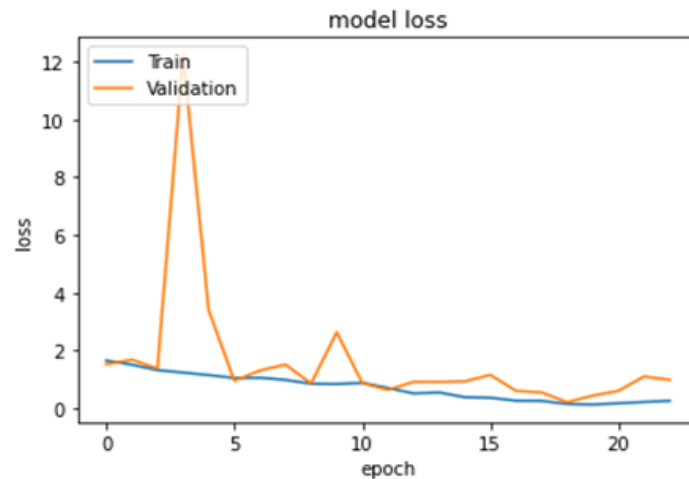


Figure 9: ResNet50 model loss for training /validation losses

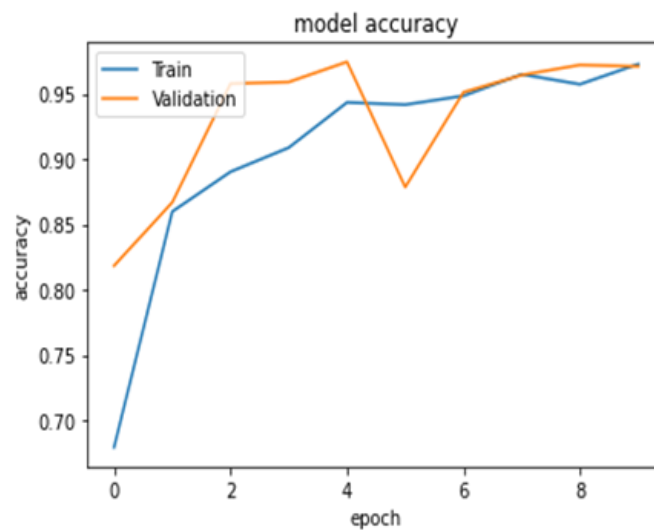


Figure 10: EfficientNetNB Model accuracy for training and validation sets

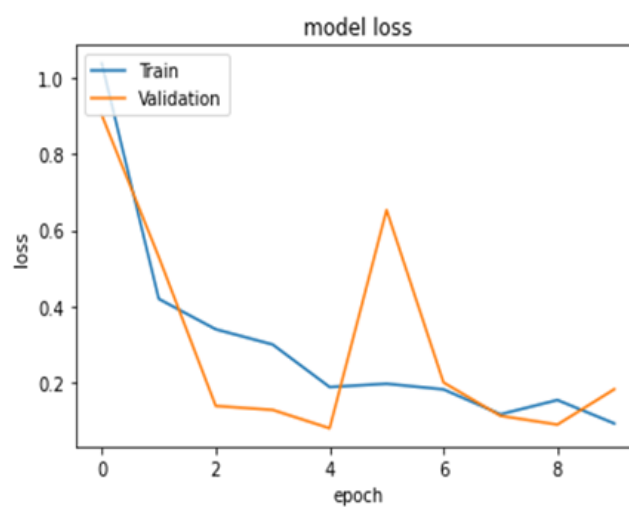


Figure 11: EfficientNetNB model loss for training validation loss

Performance and accuracy metrics are used to measure the integrity, validity, and resilience of a machine-learning model. Modeling frequently involves training a variety of

models, putting each one to use on a holdout sample, and evaluating how well it worked (James, et al., 2024d; Ekong, et al., 2024b; Ekong, et al., 2024c; James, et al., 2022). A third holdout sample dubbed the test data, is occasionally used to forecast how the selected model would perform with entirely fresh data after many models have been tested and tweaked, provided there is enough data. Fundamentally, the model evaluation procedure seeks to identify the model that generates the most reliable and practical predictions. In our dataset, skin images can be classified as true positive (Tp) or true negative (Tn) if they are detected and diagnosed accurately and can be classified into false positive (Fp) or false negative (F_n) when it misclassified. Table 2 shows the summary of the classification report.

Several techniques were employed to gauge how well various categorization algorithms utilized in the study performed, including the following;

1. **Accuracy:** Number of correctly detected instances across expressed in the following formula:

$$Accuracy = \frac{T_p + T_n}{T_p + T_n + F_p + F_n} \quad (1)$$

2. **Precision:** The predicted positive outcome concerning all expected positive outcomes expressed mathematically as:

$$Precision = \frac{T_p}{T_p + F_p} \quad (2)$$

3. **Specificity:** The model's ability to predict negative outcomes can be expressed as:

$$Specificity = \frac{T_N}{T_N + T_P} \quad (3)$$

4. **Sensitivity:** Sensitivity, similar to recall measures the strength of the model to predict a positive outcome or the proportion of the ones that it correctly identifies expressed as:

$$Sensitivity = \frac{T_p}{T_p + F_N} \quad (4)$$

5. **Recall:** Recall is the proportion of pertinent results that the algorithm correctly recognizes expressed as:

$$Recall = \frac{T_p}{T_n + F_p} \quad (5)$$

6. **F1 Score:** The harmonic mean of recall and accuracy. It is expressed as:

$$F1_{score} = 2 \times \frac{precision \times recall}{precision + recall} \quad (6)$$

7. **Area Under the Curve (AUC):** The capacity of a classifier to differentiate between classes which is a summary of the Operating Characteristic (ROC) curve. The higher the AUC, the better the model performs. It is expressed as:

$$AUC = \frac{\sum r_i(x_p) - \frac{x_p(x_p+1)}{2}}{x_p + x_n} \quad (7)$$

Where a positive and negative sample of the data is represented by x_p and x_n respectively while the rating of the positive sample is represented by r_i .

8. **(ROC-Curve):** A graphical plot illustrating the ability of a binary classifier as its discrimination threshold is adjusted.

As noted earlier, the ROC curve is only applicable to binary classification problems, however, with some tweaking, the researcher was able to modify the algorithm for multiclass classification problems.

9. Confusion Matrix: A table that categorizes accurate and inaccurate predictions. Additionally, to assess the ratio of true negatives to false negatives and true negatives, or selectivity.

Table 2: Summary of the Models' Classification Report

Models	Class	Precision	Recall	F1-Score	AUC Score	Accuracy
CNN Model (developed from scratch by researcher)	Chickenpox	0.99	0.98	0.98	0.98	0.99
	Cowpox	1.00	0.98	0.99		
	Healthy	0.98	0.99	0.99		
	Measles	0.98	0.98	0.98		
	Mpox	0.99	0.98	0.98		
	Smallpox	0.99	1.00	1.00		
ResNet50	Chickenpox	0.96	0.94	0.95	0.96	0.96
	Cowpox	0.90	0.97	0.94		
	Healthy	1.00	0.99	0.99		
	Measles	0.97	0.88	0.92		
	Mpox	0.98	0.92	0.95		
	Smallpox	0.94	0.98	0.96		
EfficientNetNB	Chickenpox	0.92	0.99	0.95	0.97	0.97
	Cowpox	0.95	1.00	0.98		
	Healthy	0.99	0.98	0.99		
	Measles	0.98	0.83	0.90		
	Mpox	0.98	0.97	0.97		
	Smallpox	0.99	0.97	0.98		

The confusion matrices evaluated using the test dataset for all three models are presented in Figure 12, Figure 13, and Figure 14 while Figure 15, Figure 16, and Figure 17 show the ROC curve for the three models highlighting different AUC scores for each class. These plots further validate the ability of our classifiers to be used for detecting and diagnosing medical diseases.

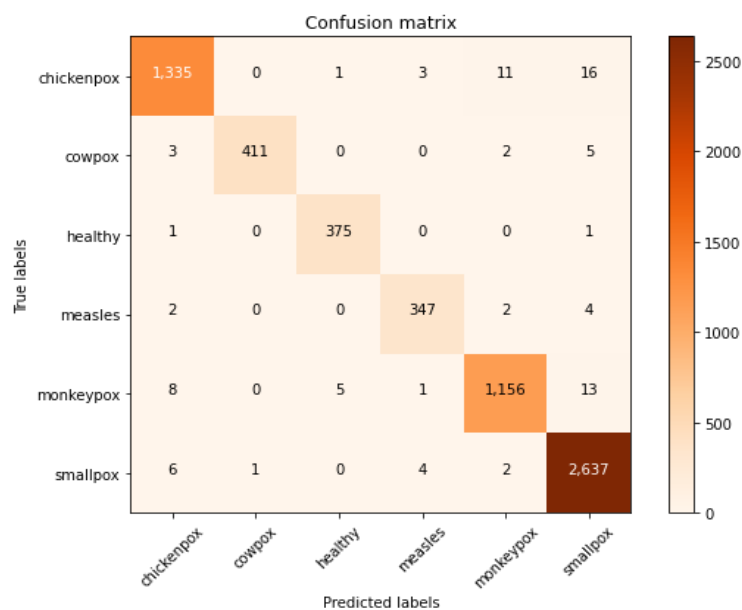


Figure 12: Confusion matrix showing predicted class and true class by the CNN model

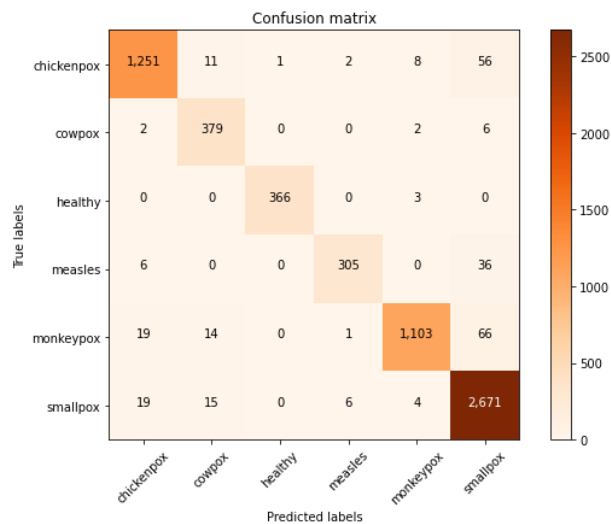


Figure 13: Confusion matrix showing predicted and true class by the ResNet50 model

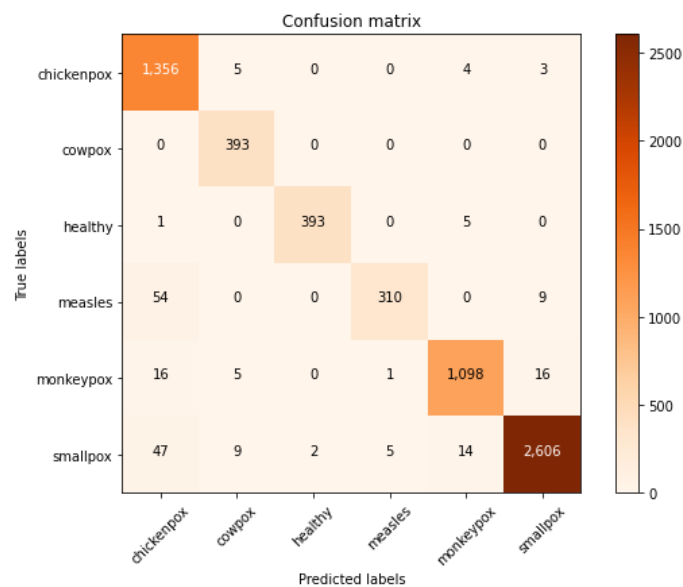


Figure 14: Confusion matrix showing predicted class and true class by the EfficientNetNB model

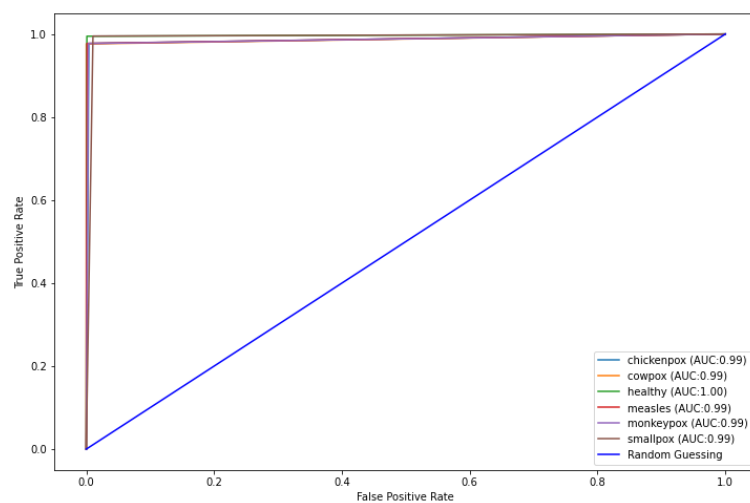


Figure 15: ROC-curve for CNN model

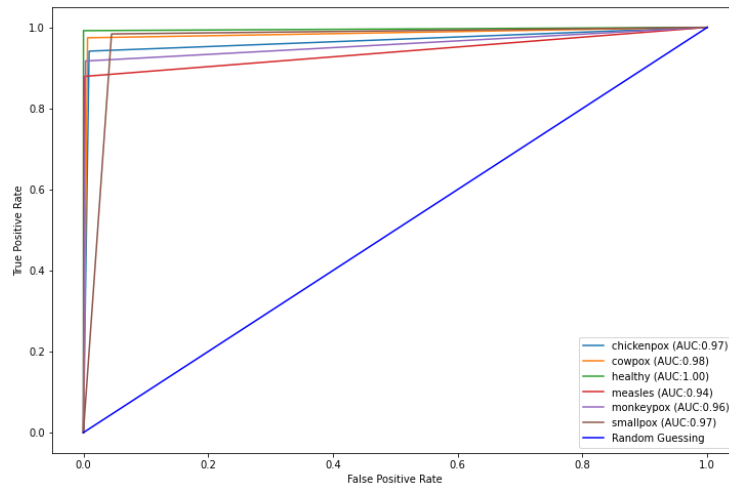


Figure 16: ROC-curve for ResNet50

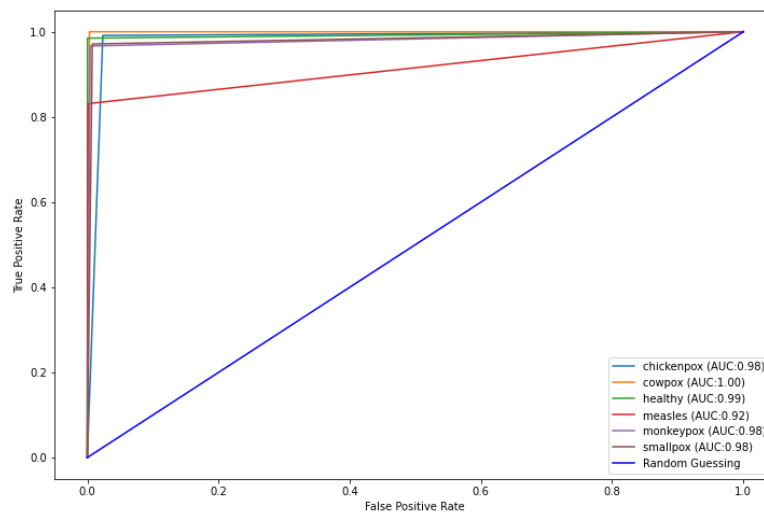


Figure 17: ROC-curve for EfficientNetNB model

Model Interpretability Using Local Interpretable Model-Agnostic Explanations (LIME)

The use of LIME to explain the detection by our deep learning models is the creation of an interpretable ML framework by Ribeiro et al. (2016). Permutations of the photos are created for explanation purposes by dividing the image into superpixels which are networks of connected, analogous-colored pixels that may be turned off by swapping out every pixel with one that the user specifies. To see just the highest contributing components in each variation sample, the user may also specify the likelihood of turning off these superpixels. Here, the use of subpixel in explaining the decision on the Mpox images is employed. The rashes on the skin as in Figure 18 are the area of interest (AOI) in our data, thus this LIME explanations identify the superpixels corresponding to these spots as having the strongest influences in deciding the prediction's conclusion. The use of LIME, as shown in Figure 19 to explain Figure 18, enables the visual tracing of the (AOI) making it simpler for those who are not specialists in the medical field to determine the patient's diagnosis.

We can notice in Figure 19 that only the super-pixels with apparent skin rashes are shown. As a result of these super-pixel components, our model has determined that our image is a skin rash caused by Mpox.

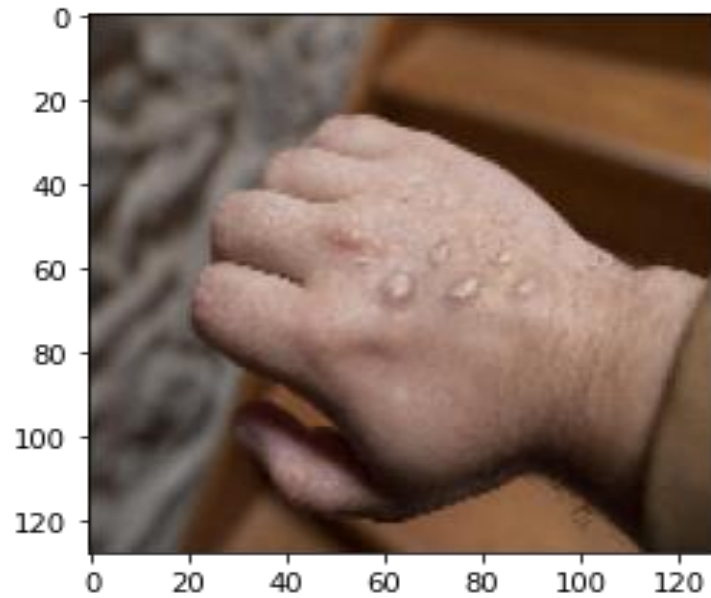


Figure 18: Input image of Mpox disease

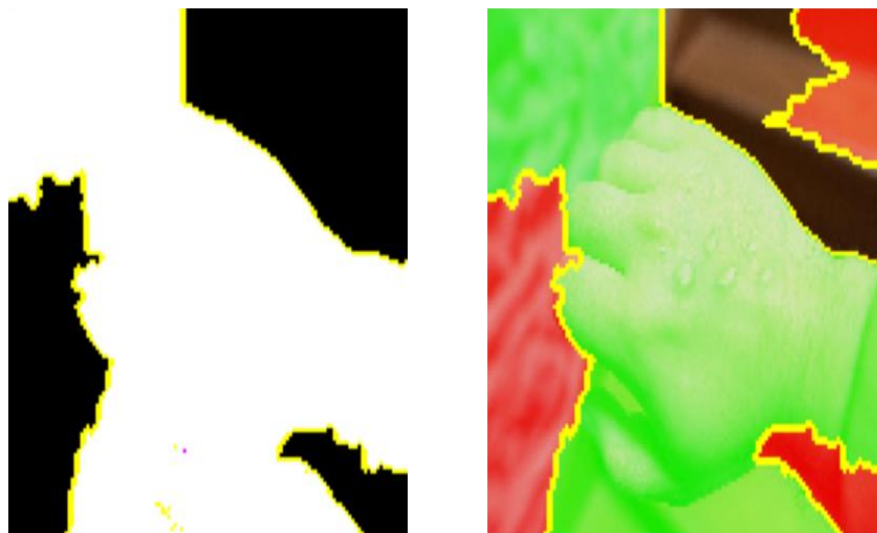


Figure 19: Classified interpretation of pox skin image in Figure 18

The area of super-pixels colored in green increases the likelihood that our image is a member of the Mpox class, whereas the area in red lowers the likelihood.

CONCLUSION

This research aimed to classify digital skin images as belonging to the Mpox virus or another class of pox virus including chickenpox, cowpox, measles, smallpox, or healthy skin images while providing meaningful insight and enhancing understanding of the decision process of the models. To achieve such a goal, dynamic and instructive data collection techniques were adopted for the development and implementation of the image dataset. Three models were deployed in this research. First, we designed and developed a convolutional neural network from scratch. Secondly, we selected two popular pre-trained state-of-the-art models with varying training parameters and used them as well for the classification to compare it with our developed model. The CNN model developed from scratch was adjudged to be the best-performing model among the three models. We obtained an accuracy of 99%, an average recall

of 99%, a precision score of 98%, an F1 score of 99%, and an AUC score of 98%. The second-best performing model was the EfficientNetNB with a 97% accuracy score, an average recall, precision, F1 score, and AUC score of 97%, 96%, 96%, and 97% respectively. The ResNet50 model was the least performing model with an accuracy score of 96% an average recall, precision, F1, and AUC score of 94%, 95%, 95%, and 96% respectively. The performance of our pre-trained models was in line with many published research works that relied on the method of transfer learning. Finally, the use of Local Interpretable Model-Agonistic Explanation was deployed to provide the solution to model explainability. LIME was used to describe the decision mechanism of the best-performing model in the prediction of MPox skin lesions, a recent requirement for the deployment of the model for clinical trials. It makes use of an efficient strategy, saving healthcare professionals both time and money. The study promotes trust in using image-based computer-aided diagnosis by assisting in the early diagnosis of the Monkeypox (Mpox) virus via insightful explanations.

REFERENCES

- Afonso, L. C. S., Rosa, G. H., Pereira, C. R., et al. (2019). A recurrence plot-based approach for Parkinson's disease identification. *Future Generation Computing System*, 94, 282–292.
- Ahmad, M. A., Eckert, C., & Teredesai, A. (2018, August). Interpretable machine learning in healthcare. In *Proceedings of the 2018 ACM international conference on bioinformatics, computational biology, and health informatics* (pp. 559-560).
- Ahsan, M., Uddin, M., Farjana, M., Sakib, A., Momin, K., & Luna, S. (2022). *Image data collection and implementation of the deep learning-based model in detecting mpox disease using modified vgg16*. arXiv preprint arXiv:2206.01862.
- Ali, S., Ahmed, M., Paul, J., Jahan, T., Sani, S., Noor, N., & Hasan, T. (2022). *Mpox skin lesion detection using deep learning models: feasibility study*, arXiv preprint arXiv:2207.03342.
- Allugunti, V. (2022). Breast cancer detection based on thermographic images using machine learning and deep learning algorithms. *Engineering in Computer Science*, 4(1), 49-56.
- CDC (2022). *Monitoring People Who Have Been Exposed*. Retrieved October 4, 2022 from <https://www.cdc.gov/poxvirus/mpox/clinicians/monitoring.html>.
- Das, D., Ito, J., Kadowaki, T., & Tsuda, K. (2019). An interpretable machine learning model for diagnosis of Alzheimer's disease. *PeerJ*, 7, e6543. <https://doi.org/10.7717/peerj.6543>.
- Ekong, A. (2023). Evaluation of machine learning techniques towards early detection of cardiovascular diseases. *American Journal of Artificial Intelligence*, 7(1), 6-16.
- Ekong, A., Ekong, B., & Edet, A. (2022). Supervised machine learning model for effective classification of patients with Covid-19 symptoms based on Bayesian belief network. *Researchers Journal of Science and Technology*, 2022(2), 27 – 3.
- Ekong, A. P., James, G. G., & Ohaeri, I. (2024a). Oil and gas pipeline leakage detection using IoT and deep learning algorithm. *Journal of Information Systems and Informatics*, 6(1), 421-434.
- Ekong, A., Attih, I., James, G., & Edet, U. (2024b). Effective classification of diabetes mellitus using support vector machine algorithm. *Researchers Journal of Science and Technology*, 4(2), 18-34.
- Ekong, A., James, G., Ekpe, G., Edet, A., & Dominic, E. A. (2024c). Model for the Classification of Bladder State Based on Bayesian Network. *International Journal of Engineering and Artificial Intelligence*, 5(2), 33-47.
- Fujita, H. & Cimr, D. (2019). Computer Aided detection for fibrillations and flutters using deep convolutional neural network. *Information Science*, 486, 231–239.

- Gao, J., Jiang, Q., Zhou, B., & Chen, D. (2019). Convolutional neural networks for computer-aided detection or diagnosis in medical image analysis: An overview. *Mathematical biosciences and engineering: MBE*, 16(6), 6536–6561. <https://doi.org/10.3934/mbe.2019326>
- González-Díaz, I. (2019). DermaKNet: Incorporating the Knowledge of Dermatologists to Convolutional Neural Networks for Skin Lesion Diagnosis. *IEEE Journal of Biomedical and Health Informatics*, 23(2), 547-559. doi: 10.1109/JB-HI2018.2806962.
- Hosseini-Asl, E., Ghazal, M., Mahmoud, A., Aslantas, A., Shalaby, A., Casanova, M., Barnes, G., Gimel'farb, G., Keynton, R., & El-Baz, A. (2018). Alzheimer's disease diagnostics by a 3D deeply supervised adaptable convolutional network. *Frontiers in bioscience (Landmark edition)*, 23(3), 584–596. <https://doi.org/10.2741/4606>
- James, G. G., Okpako, A. E., Ituma, C., & Asuquo, J. E. (2022). Development of Hybrid Intelligent based Information Retrieval Technique. *International Journal of Computer Applications*, 975, 8887. doi: 10.5120/ijca2022922401.
- James, G., Ekong, A., & Odikwa, H. (2024a). Intelligent model for the early detection of breast cancer using fine needle aspiration of breast mass. *International Journal of Research and Innovation in Applied Science, IX (III)*, 348-359. doi: 10.51584/IJRIAS.2024.90332.
- James, G. G., Oise, G. P., Chukwu, E. G., Michael, N. A., Ekpo, W. F., & Okafor, P. E. (2024b). Optimizing business intelligence system using big data and machine learning. *Journal of Information Systems and Informatics*, 6(2), 1215-1236. <http://journal-isi.org/index.php/isi>.
- James, G. G., Okafor, P. C., Chukwu, E. G., Michael, N. A., & Ebong, O. A. (2024c). Predictions of criminal tendency through facial expression using convolutional neural network. *Journal of Information Systems and Informatics*, 6(1), 13-29. <http://journal-isi.org/index.php/isi>.
- James, G., Umoren, I., Ekong, A., Inyang, S., & Aloysius, O. (2024d). Comparative analysis of support vector machine and random forest models for classification of the impact of technostress in covid and post-covid era.
- Jeyaraj, P. & Samuel Nadar, E. (2019). Computer-assisted medical image classification for early diagnosis of oral cancer employing deep learning algorithm. *Journal of cancer research and clinical oncology*, 145(4), 829–837. <https://doi.org/10.1007/s00432-018-02834-7>
- Lundberg, S.M. & Lee, S.I. (2017). A unified approach to interpreting model predictions. *Advances in Neural Information Processing Systems*, 4765–4774.
- Lundervold, A. & Lundervold, A. (2019). An overview of deep learning in medical imaging focusing on MRI. *Zeitschrift für Medizinische Physik*, 29(2), 102–127. <https://doi.org/10.1016/j.zemedi.2018.11.002>
- Magesh, P. R., Myloth, R. D., & Tom, R. J. (2020). An explainable machine learning model for early detection of Parkinson's disease using LIME on DaTSCAN imagery. *Computers in Biology and Medicine*, 126, 104041.
- Muñoz-Saavedra, L., Escobar-Linero, E., Civit-Masot, J., Luna-Perejón, F., Civit, A., & Domínguez-Morales, M. (2022). Monkeypox diagnostic-aid system using CNNs. *Sensors*, 1.
- Naseem, U., Rashid, J., Ali, L., Kim, J., Haq, Q. E. U., Awan, M. J., & Imran, M. (2022). An automatic detection of breast cancer diagnosis and prognosis based on machine learning using ensemble of classifiers. *IEEE Access*, 10, 78242-78252.
- NCDC (2022). *Update on Monkeypox (MPX) in Nigeria. Situation report, August 2022* Retrieved September, 30, 2022 from <https://ncdc.gov.ng/themes/common/files/sitreps/df7aef34e7951daceb1f957501ea3374.pdf>

- Petsiuk, V., Das, A., & Saenko, K. (2018). *Rise: Randomized Input Sampling for Explanation of Black-Box Models*. arXiv preprint arXiv:1806.07421.
- Raghavendra, U., Fujita, H., & Bhandary, S. V. (2018). Deep convolution neural network for accurate diagnosis of glaucoma using digital fundus images. *Information. Science*, 441, 41–49.
- Ribeiro, M., Singh, S., & Guestrin, C. (2016). Why should I trust you? Explaining the predictions of any classifier. *Proceedings of the 22nd ACM SIGKDD. International Conference on Knowledge Discovery and Data Mining*, 1135–1144.
- Shchelkunov, S. N., Totmenin, A. V., Safronov, P. F., Mikheev, M. V., Gutorov, V. V., Ryazankina, O. I., ... & Moss, B. (2002). Analysis of the monkeypox virus genome. *Virology*, 297(2), 172-194. <https://doi.org/10.1006/viro.2002.1446>.
- Shi, Z., Hao, H., Zhao, M., Feng, Y., He, L., Wang, Y., & Suzuki, K. (2019). A deep CNN based transfer learning method for false positive reduction. *Multimedia Tools and Applications*, 78, 1017-1033.
- Xu, R., Wang, Z., Liu, Z., Han, C., Yan, L., Lin, H., ... & Liu, Z. (2022). Histopathological tissue segmentation of lung cancer with bilinear CNN and soft attention. *BioMed Research International*, 2022(1), 7966553. doi: 10.1155/2022/7966553.
- Zhao, X., Liu, L., Qi, S., Teng, Y., Li, J., & Qian, W. (2018). Agile convolutional neural network for pulmonary nodule classification using CT images. *International journal of computer-assisted radiology and surgery*, 13(4), 585–595. <https://doi.org/10.1007/s11548-017-1696-0>
- Zhou, Y. J., Xu, J. X., & Liu, Q. G. (2018). A Radiomics Approach with CNN for Shear-wave Elastography Breast Tumor Classification. *IEEE Transactions on Biomedical Engineering*, 65(9), 1935–1942.